Scour at Culvert Outlets in Multibed Materials

STEVEN R. ABT, JAMES F. RUFF, AND CESAR MENDOZA

An investigation of scour at culvert outlets in noncohesive and SC-type cohesive materials is presented. A series of empirical equations was derived to predict the depth, width, length, and volume of scour downstream of culvert outlets under various field and laboratory conditions. The rate of scour was determined for each material. The effects of culvert shape, tailwater depth, and headwall presence were correlated with the ultimate scour dimensions. The area affected by the scour process was quantified as a function of culvert diameter and discharge. General observations on scour-hole formation, growth, and stabilization are reported.

One of the major considerations in the design and construction of a roadway system is the conveyance of tributary drainage through the roadway embankment. As drainage waters are conveyed through the embankment, flow discharges from the culvert and impinges on the material beneath the outlet. The impinging jet lifts the material particles and transports those particles downstream of the impact area. The jet impact area is transformed into an energy dissipator, and a hole is created at the outlet. The eventual result of this scour and erosive process, if it is left unchecked, is degradation of the roadway embankment, degradation of the area beneath and adjacent to the culvert outlet, and aggradation of the channel, land areas, or properties downstream of the outlet. Because of these severe and often costly damages, the study of localized scour is an important step in the evaluation, control, and management of roadway embankment erosion.

The investigation of scour at culvert outlets has continued for several decades. Early studies, beginning with Rouse (1) and Laursen (2), attempted to understand the general nature and principles of scour. Scour was observed to be a function of discharge, time, and material characteristics. A number of investigations have identified the significant characteristics of localized scour at culvert outlets. These studies address the following general topics: the effects of falling jets (3) and the degree of armor plating in gravel bed materials (4); the effect of headwalls on predicting scour in sand bed materials (5); the effects of material shape (6), tailwater (7,8), and jet impingement on riprap materials (9); and the prediction of scour in a cohesive material (10). In most cases emphasis is placed on predicting the extent and dimensions of the degradation processes.

The most notable studies were those of Bohan (7) and Fletcher and Grace (11) of the U.S. Army Engineer Waterways Experiment Station. They formulated a series of empirical equations that predicted the length, depth, width, and volume of scour as a function of discharge, culvert diameter, and time. Bohan and Fletcher and Grace realized the significant effect of tailwater conditions on ultimate scour-hole dimensions. Therefore, their prediction equations were generalized to encompass a spectrum of tailwater conditions. Although several studies followed the investigations of Bohan and Fletcher and Grace, their work has been adopted as the most comprehensive design criteria available for the prediction of scour-hole dimensions.

The ability to predict the magnitude and geometry of localized scour and subsequent deposition at culvert outlets is a useful evaluation tool in the control and management of erosion along roadway embankments. However, because previously developed equations are considered conservative, it is advantageous to investigate localized scour in noncohesive and cohesive materials at culvert outlets.

EXPERIMENTAL FACILITIES AND PROCEDURES

In the investigation of scour at culvert outlets in mixed-bed materials, five materials were used under a variety of conditions. Materials were tested in two facilities with culverts ranging in diameter from 4 to 18 in. (10.2 to 45.7 cm). Test periods ranged from 316 to 1000 min in duration and discharges ranged from 0.11 to 29.13 ft^3/sec (0.003 to 0.83 m^3/sec). A summary of the experimental materials, models, discharges, and test durations is given in Table 1.

Experimental Facilities

Two hydraulic flumes were used for conducting the scour investigation. The initial testing program was conducted in an outdoor concrete flume 100 ft (30.5 m) long, 20 ft (6.1 m) wide, and 8 ft (2.4 m) deep. A smooth pipe (culvert) was horizontally cantilevered through the headwall between the sidewalls and extended approximately 6 ft (1.9 m) into the test section. Bed material was placed adjacent to the pipe invert and leveled with a minimum thickness of 6 ft.

The scope of the study was expanded to incorporate a smaller indoor flume 15 ft (4.5 m) long, 4 ft (1.2 m) wide, and 2 ft (0.6) deep. The indoor facility was a 1:5 Froude scale model of the outdoor flume.

Description of Bed Materials

Four noncohesive materials and one cohesive soil were used as bed materials for the scour investigation. The soil properties of each bed material were obtained and recorded in accordance with procedures outlined in ASTM specifications.

Noncohesive Materials

The four noncohesive materials tested included a uniform sand, a uniform gravel, a graded sand, and a graded gravel. The soil properties of the noncohesive material are summarized in Table 2. The specific gravity of the noncohesive material source was determined to be 2.65.

Cohesive Bed Material

The cohesive material was derived from a residual Colorado expansive clay mixed with a graded sand. The tan-green sandy clay mixture is classified as an SC soil type in accordance with the Unified Soil Classification system. An agricultural analysis further categorized the material as a sandy loam composed of 58 percent sand, 27 percent clay, and 15 percent silts and organic matter. The cohesive material properties are summarized in Table 3.

Test Procedure

The bed was leveled adjacent to the culvert invert elevation. Water was directed from the water source

Table 1. Test program parameters.

Material	d_{50} (mm)	Model (ft)	Pipe Diameter (in.)	Discharge Range (ft^3/sec)	Times of Data Collection (mins)	Tailwater Elevation[a]
Uniform sand	1.86	20	4	0.11- 1.14	31,100,316	0.45
		20	7	1.15- 7.65	31,100,316	0.00
		20	7	1.15- 7.65	31,100,316	0.25
		20	7	1.89- 9.45	31,100,316,1000	0.45
		20	13.5	3.85-19.26	31,100,316,1000	0.45
		20	17.5	7.31-29.23	31,100,316,1000	0.45
		4[b]	4	0.16- 0.91	31,100,316,1000	0.45
		4[c]	4	0.16- 0.91	31,100,316,1000	0.45
		4	4x4	0.25- 1.16	31,100,316	0.45
Graded sand	2.0	4	4	0.18- 0.73	31,100,316	0.45
Uniform gravel	7.62	20	3	1.91- 7.65	31,100,316	0.0
		20	3	1.91- 7.65	31,100,316	0.25
		20	3	1.91- 7.65	31,100,316	0.45
Graded gravel	7.34	20	7	1.91- 7.65	31,100,316	0.45
Cohesive	0.15	20	7	1.91- 7.65	31,100,316,1000	0.45
		20	13.5	3.81-15.23	31,100,316,1000	0.45
		20	16	7.28-29.13	31,100,316,1000	0.45

[a]Water depth as a portion of culvert diameter.
[b]Without headwall.
[c]With headwall.

Table 2. Properties of noncohesive materials.

Soil Type	d_{50} (mm)	Standard Deviation[a]	Unit Weight (lb/ft^3)	Angle of Repose (°)	Fall Velocity (cm/sec)
Uniform sand (medium)	1.86	1.33	93.8	34.8	27.1
Graded sand	2.00	4.38	105.9	31.8	27.3
Uniform gravel	7.62	1.32	94.4	37.3	63.0
Graded gravel	7.34	4.78	117.9	37.3	64.0

[a]Standard deviation (σ) is $(d_{84}/d_{16})^{0.5}$

Table 3. Properties of cohesive materials.

Characteristic	Characteristic Value
Soil type	SC
Texture	Sandy loam
Atterberg limits	
Liquid limit	34
Plastic limit	19
Plastic index	15
Soil composition (%)	
Organic matter	1
Sand	58
Silt	14
Clay	27
pH	7.8
Mean grain size (mm)	0.15
Uniformity coefficient	300
Fall velocity (d_{50}) (ft/sec)	0.08
Cation exchange capacity (meq/100g)	9.0
Soil fabric	Dispersed
Dispersivity of colloid fraction	Nondispersive
Permeability (cm/sec)	6.4×10^{-6}

to a sump located downstream of the material testing basin until the water reached the desired tailwater elevation. The control valve was gradually opened until the discharge reached the desired level. The tailwater elevation was adjusted and maintained above the bed at levels given in Table 1.

In general, scour profiles were taken after predetermined time periods measured from the beginning of each test. The model bed was mapped by using a point gauge.

Discharge Intensity

The Froude number of circular sections $(\bar{V}g^{-0.5}D^{-0.5})$ was modified to $Qg^{-0.5}D^{-2.5}$, where $V = Q/A$ and $A = \pi D^2/4$. This form of the Froude number is referred to as the discharge intensity (DI).

RESULTS AND DISCUSSION

General Observations

Noncohesive Materials

A series of 75 scour tests was conducted, observed, and documented as water discharged from a culvert outlet onto a bed of noncohesive materials. Scour holes were generally similar in geometric configuration and appearance. They were circular in shape at low DI ($DI \leq 1.0$) and elongated to an oval shape as the DI exceeded 1 ($DI > 1.0$).

Scour holes were created by a water jet striking a horizontal bed of noncohesive material. The force of the jet and subsequent turbulence lifted and entrained the material particles. Large-diameter materials were transported as bed load along the bottom of the scour hole and along bed downstream of the hole. Smaller materials were entrained by the flow and deposited around the rim of the hole, in the subsequent dune or mound downstream from the hole, or in the material settling basin. The mounds that formed were fan-shaped for $DI < 1.0$ and became elongated as the DI reached 1 ($DI \geq 1.0$). The surface of the mounds was flat, paralleling the water surface. The mound height was generally observed to be approximately 0.6 to 0.8 of the tailwater depth.

Cohesive Material

A series of 12 scour holes was observed and documented for the cohesive bed material. The scour holes were generally similar in geometric configuration. Scour holes were circular in shape at low DI ($DI \leq 1.0$). As the DI increased ($DI > 1.0$), the holes elongated to an oval shape.

The force of the water jet striking the bed weakened the cohesive bonds of the material and dislodged particles from the bed. The material was then lifted and entrained into the turbulent flow. Large-diameter materials (sands and clods) were transported as bed load along the bottom of the scour cavity and deposited immediately downstream of the jet impact area. A mound subsequently formed downstream of the cavity. The smaller materials (clay and silt particles) were entrained by the flow

and trapped in void spaces along the mound or transported to the material settling basin. Each mound was generally flat, less than 0.25D in height, and fan-shaped downstream of the cavity. The mound was primarily composed of large-diameter sands and clods and fine material filling the void spaces.

Considerable deposition of sands and clods was observed around the rim of the hole at the conclusion of each experiment. This apparent armoring effect consistently occurred at the downstream face and along the rim of all scour holes. Limited armoring was observed within the scour hole. Armoring materials could not be supported along the cavity walls due to steep sideslopes and vertical sidewalls. In some cases cantilevering occurred.

Quantitative Results

After the scour tests were completed, an analysis was conducted to correlate the depth, width, length, and volume of scour with materials, culvert, and discharge. Scour-hole depth, width, length, and volume are expressed by the following dimensionless parameters:

Characteristic	Parameter
Depth	d_{sm}/D
Width	W_{sm}/D
Length	L_{sm}/D
Volume	V_{sm}/D^3

The relationships presented here are based on the maximum scour-hole dimensions. Test durations were in accordance with the times given in Table 1.

Graphical representations were compiled correlating the dimensionless depth, width, length, and volume parameters with DI, as shown in Figure 1 for uniform sand (d_{50} = 1.86, σ = 1.33, and t_o = 1000 min). A power regression line was fit through each logarithmic plot, which yielded a series of expressions of the following general form:

$$y = a\,x^b \tag{1}$$

where

y = dependent variable of d_{sm}/D, W_{sm}/D, L_{sm}/D, or V_{sm}/D^3;
a = a constant; and
b = slope of the linearized plot.

From these expressions it was evident that the maximum scour-hole characteristics of depth, width, length, and volume can be correlated with the culvert diameter (D) and culvert discharge (Q). Replacing the independent variable of Equation 1 with the DI yields the following expression for d_{sm}/D or any of the other dimensionless parameters:

$$d_{sm}/D = a\,(Q/g^{1/2}\,D^{5/2})^b \tag{2}$$

The DI relationships yield a conservative estimate of scour-hole dimensions for partly filled culverts (DI < 1.0).

A number of empirical relationships were similarly formulated for the cohesive soil correlating the four maximum dimensionless scour characteristics with the inverted shear number (S_η), as shown in Figure 2. The inverted shear number is

$$S_\eta = \rho\bar{V}^2/\tau_c \tag{3}$$

where the critical shear stress (τ_c) is

$$\tau_c = 0.001\,(S_v + 130)\tan(30 + 1.73\,I_p) \tag{4}$$

The maximum scour-hole depth, width, length, and volume can be correlated with D, average velocity of fluid at the culvert outlet ($\bar{V}$), fluid density (ρ), saturated soil shear stress (S_v), and soil plasticity index (I_p). Replacing the independent variable of Equation 2 with the inverted shear number yields the following equation for any of the four dimensionless parameters:

$$d_{sm}/D = a\,(\rho\bar{V}^2/\tau_c)^b \tag{5}$$

Figure 1. Dimensionless scour-hole parameters versus DI for uniform sand, where d_{50} = 1.86 mm, σ = 1.33, and t_o = 1,000 min.

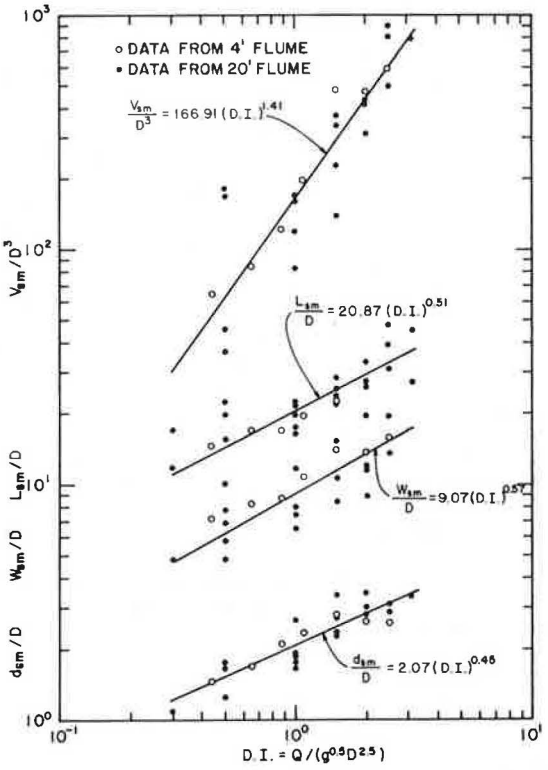

Figure 2. Characteristic dimensions of scour versus inverted shear number.

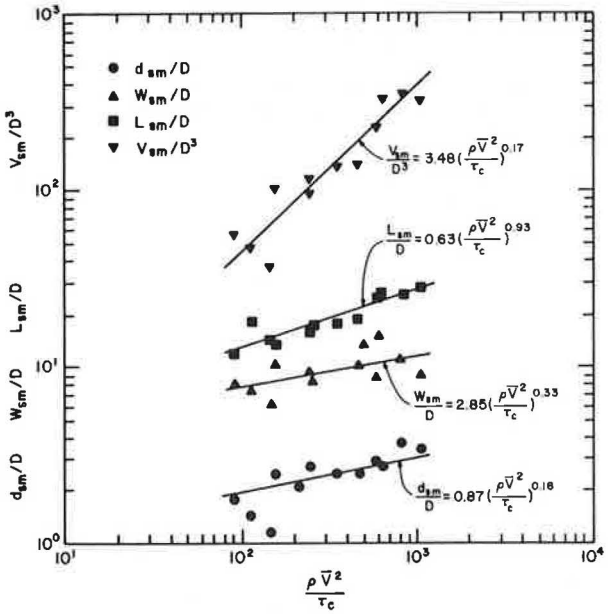

Time Relationships

Scour-hole measurements were taken at 31, 100, and 316 min for all of the noncohesive materials; a portion of the uniform sand tests and all of the cohesive soil tests extended to 100 min in duration. The observed scour-hole characteristics were evaluated for each time interval. Characteristic values were normalized with reference to the final or maximum values obtained after the appropriate test durations.

After 31 min of testing, a minimum of 80.0 percent of the 316-min scour depth was attained independent of the type of material tested. Furthermore, the 31-min values for scour-hole width, length, and volume averaged 83, 80, and 61 percent of the 316-min values, respectively. The 31-min rate of scour of the cohesive material was close to the average 31-min rate of scour of the noncohesive materials.

A comparison of the 316-min scour-hole dimensions with the 1000-min scour-hole dimensions indicates that, although the duration of scour extended 684 min (216 percent) longer, the scour-hole dimensions increased on an average by 14 percent in depth, 7 percent in width, 16 percent in length, and 46 percent in volume.

Logarithmic plots of normalized scour-hole characteristics versus normalized time (t/t_o) are shown in Figure 3. In this case, t is any time less than or equal to the duration of scour (t_o). By using the power relationship depicted in Equation 1, a number of regression curves were fit to the data where time is the independent variable.

Scour Relationships

By using the dimensionless parameters and characteristic relationships developed thus far, it is possible to formulate equations that estimate scour-hole dimensions at any finite time between 31 min and the test duration of 316 to 1000 min. Combining Equation 1 with the time expression yields an equation that relates a desired hole characteristic to its maximum value as a function of time. The resulting equation is

$$y = a\,(x)^b * (t/t_o)^c \qquad (6)$$

Figure 3. Normalized scour-hole characteristics versus normalized time for uniform sand.

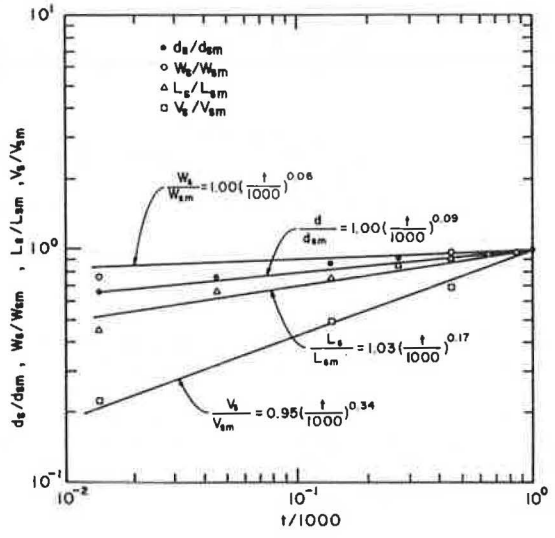

where

a = a coefficient;
b = slope of the desired characteristic curve;
c = slope of the desired time relationship;
x = independent variable of $Qg^{-0.5}\,D^{-2.5}$ or $\rho V^2(\tau_c)^{-1}$; and
y = dependent variable of d_s/D, W_s/D, L_s/D, or V_s/D^3.

Furthermore, because some of the tests were run for a 316-min duration and others were run for 1000 min, the coefficient a can be multiplied by the appropriate time normalization percentages to ensure that all of the materials will have the same divisor for the time parameter.

Table 4 gives a summary of the coefficients and exponents for each material and scour-hole parameter. Exponents b and c are the same as the component regression analyses for each independent variable. The coefficients a are the product of the coefficients from the component regression analyses for each independent variable times the normalization percentages d_{s316}/d_{s1000}, W_{s316}/W_{s1000}, L_{s316}/L_{s1000}, and V_{s316}/V_{s1000} for the runs that extended to 1000 min.

A compilation of maximum scour-hole depths versus DI for four uniform materials and two graded materials is shown in Figure 4.

Tailwater Effects

Tests were run to investigate further the effects of tailwater (TW) depth on scour-hole dimensions. Previous tests by Bohan (7) and Fletcher and Grace (11) of the U.S. Army Corps of Engineers demonstrated that maximum scour occurred when TW was below the culvert center line. Tests were run at TW of zero, 0.25D, and 0.45D to determine where scour tended to be the greatest.

The depth, width, length, and volume of scour were correlated with the DI for each TW elevation as in the plots shown in Figure 5. Little difference in scour is observed between zero TW and 0.25D TW for the sand bed material. As the tailwater was raised from 0.25D to 0.45D, the depth and width of scour decreased while the length and volume of scour increased. Overall, scour-hole dimensions at 0.25D TW were no more than 10 percent greater than tests at 0.45D TW. Little difference was observed in the maximum scour-hole dimensions as the TW varied from zero to 0.45D for DIs of $\geq$1.5.

Effects of Culvert Shape

Test runs were performed to investigate how the shape of a culvert affected scour-hole depth, length, and volume. Only circular and square culverts were considered in this analysis.

Culverts were sized so that the diameter of the circular culvert was equivalent to the length of one side of the square culvert. Because the cross-sectional areas of the two culverts were not identical, it was necessary to compare the results based on parameters other than DI and D.

Analyses were performed by using an equivalent depth parameter (Y_e). The equivalent depth is a characteristic length applicable to culverts of any shape and is expressed as

$$Y_e = (A/2)^{1/2} \qquad (7)$$

where A is the cross-sectional area of flow.

A comparison of equivalent depth with three of the dimensionless scour-hole parameters--d_{sm}/Y_e, L_{sm}/Y_e, and $V_{sm}/Y_e{}^3$--is shown in Figure 6. It is observed

Table 4. Equation coefficients and exponents in terms of constant 316-min duration.

Material	d_{50} (mm)	σ	Dependent Variable (y)	Independent Variable (x)	a	b	c
Uniform sand	1.86	1.33	d_s/D	$Qg^{-0.5}D^{2.5}$	1.86	0.45	0.09
			W_s/D	$Qg^{-0.5}D^{2.5}$	8.44	0.57	0.06
			L_s/D	$Qg^{-0.5}D^{2.5}$	18.28	0.51	0.17
			V_s/D^3	$Qg^{-0.5}D^{2.5}$	101.48	1.41	0.34
Graded sand	2.00	4.38	d_s/D	$Qg^{-0.5}D^{2.5}$	1.22	0.82	0.07
			W_s/D	$Qg^{-0.5}D^{2.5}$	7.25	0.76	0.06
			L_s/D	$Qg^{-0.5}D^{2.5}$	12.77	0.41	0.04
			V_s/D^3	$Qg^{-0.5}D^{2.5}$	36.17	2.09	0.19
Uniform gravel	7.62	1.32	d_s/D	$Qg^{-0.5}D^{2.5}$	1.78	0.45	0.04
			W_s/D	$Qg^{-0.5}D^{2.5}$	9.13	0.62	0.08
			L_s/D	$Qg^{-0.5}D^{2.5}$	14.36	0.95	0.12
			V_s/D^3	$Qg^{-0.5}D^{2.5}$	65.91	1.86	0.19
Graded gravel	7.34	4.78	d_s/D	$Qg^{-0.5}D^{2.5}$	1.49	0.50	0.03
			W_s/D	$Qg^{-0.5}D^{2.5}$	8.76	0.89	0.10
			L_s/D	$Qg^{-0.5}D^{2.5}$	13.09	0.62	0.07
			V_s/D^3	$Qg^{-0.5}D^{2.5}$	42.31	2.28	0.17
Cohesive sandy clay		0.15	d_s/D	$Qg^{-0.5}D^{-2.5}$	1.86	0.57	0.10
			W_s/D	$Qg^{-0.5}D^{-2.5}$	8.63	0.35	0.07
			L_s/D	$Qg^{-0.5}D^{-2.5}$	15.30	0.43	0.09
			V_s/D^3	$Qg^{-0.5}D^{-2.5}$	79.73	1.42	0.23
Cohesive sandy clay		0.15	d_s/D^3	$\rho V^2 \tau_c^{-1}$	0.86	0.18	0.10
			W_s/D	$\rho V^2 \tau_c^{-1}$	3.55	0.17	0.07
			L_s/D	$\rho V^2 \tau_c^{-1}$	2.82	0.33	0.09
			V_s/D^3	$\rho V^2 \tau_c^{-1}$	0.62	0.93	0.23

Note: Modified equation: $y = a\,(x)^b * (t/316\ \text{min})^c$, where $t \leq 1000$ min and $t \geq 31$ min.

Figure 4. d_{sm}/D versus DI for cohesive and noncohesive material (curves adjusted to common time base of 316 min).

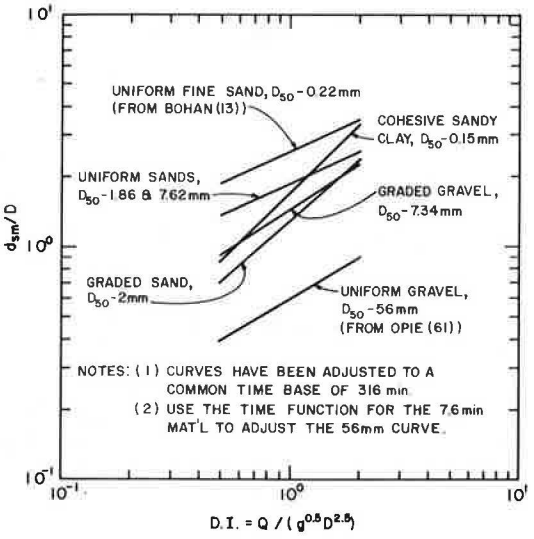

Figure 5. Tailwater comparison of scour-hole depth and length versus DI for uniform sand.

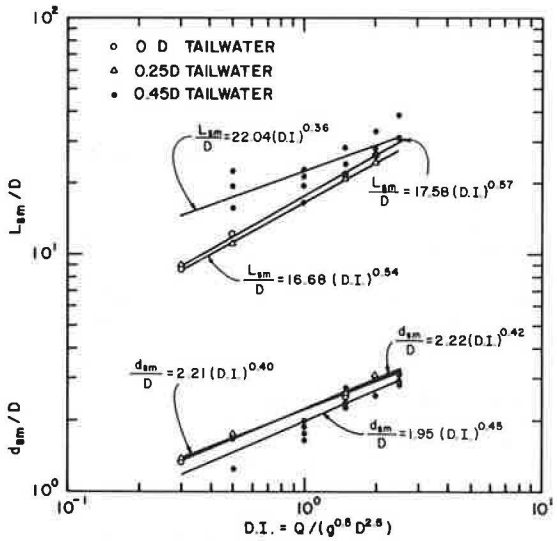

that the dimensions of scour are greater for circular-shaped culverts than for square-shaped culverts of similar characteristic lengths.

The Froude relationship was also selected for analysis where the Froude number (F) is defined as

$$F = \overline{V}/\sqrt{gL} \tag{8}$$

where g is the acceleration of gravity and L is the culvert characteristic length. The hydraulic radius (R_H) was selected as a common-denominator characteristic length and is defined as

$$R_H = A/WP \tag{9}$$

where A is the cross-sectional area of flow and WP is the wetted perimeter.

The Froude number was compared with the dimensionless scour-hole parameters of d_{sm}/R_H, L_{sm}/R_H, and V_{sm}/R_H^3. Figure 6 shows the dimensions of scour to be greater for circular-shaped culverts than for square-shaped culverts of similar characteristic lengths. Froude numbers varied from 2 to 6.5.

An analysis was performed to evaluate which parameter, equivalent depth, or Froude number more closely predicted scour-hole dimensions when culverts were flowing full. The resulting equations, using the equivalent-depth analysis, yield a conservative estimate of scour-hole dimensions at low DI (DI < 1.0) and tend to underestimate scour-hole dimensions at higher DI (DI $\geq$ 1.5).

It was observed that as the flow discharged from the square outlet the jet dispersed and impacted over a wider area than the more concentrated jet from the circular culvert. Therefore, it is anticipated that the estimated depth of scour will be less for rectangular culverts than that predicted for

Figure 6. Equivalent-depth comparison of circular- and square-shaped culverts for uniform sand.

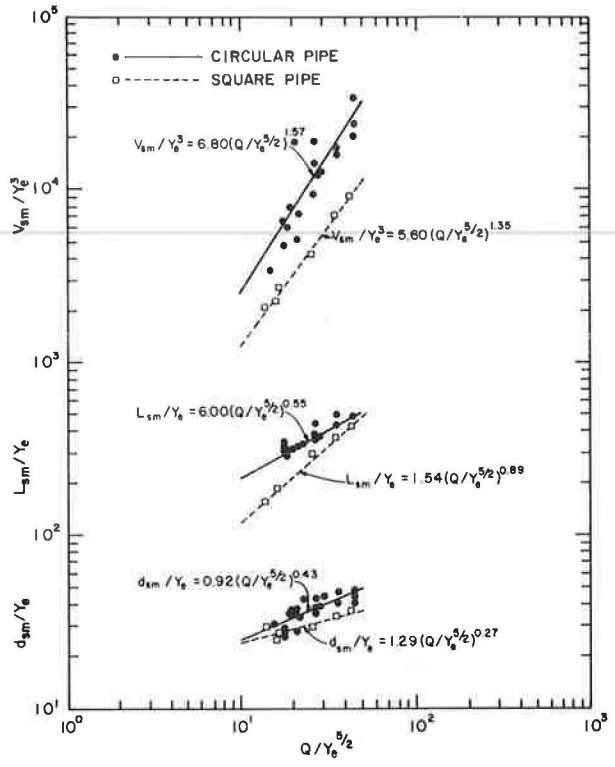

circular- and square-shaped culverts at identical Froude numbers. In this case, the culvert height is used as the characteristic length.

These test results indicate that circular-shaped culverts yield more conservative scour-hole dimensions than square-shaped culverts of similar characteristic lengths. A Froude number analysis using the hydraulic radius and equivalent-depth analysis can be used to predict scour-hole dimensions adequately at all DIs.

Headwall Effects and Scour Profiles

Tests were performed by placing a headwall adjacent to the culvert outlet in the uniform sand material. The scour-hole dimensions were compared with tests performed under similar conditions without the headwall. The test results for conditions with and without headwalls are shown in Figure 7. The results indicate that little difference exists in the scour-hole dimensions for the two conditions.

Dimensionless profiles of the scour-hole centerline are shown in Figure 8 for conditions with and without headwalls. The profiles indicate that the scour-hole depth and length downstream of the culvert outlet are approximately the same with and without a headwall. The maximum depth of scour was observed at a point between approximately $0.3L_{sm}$ and $0.43L_{sm}$ downstream of the culvert outlet, where L_{sm} is the maximum length of scour. Erosion was observed directly under the culvert outlet to be approximately $0.4d_{sm}$, where d_{sm} is the maximum scour depth for the no-headwall condition. Furthermore, undermining of the culvert often extended $0.2L_{sm}$ into the embankment from the culvert outlet without the headwall.

Figure 8 shows that, if a headwall is installed at the culvert outlet, scour can extend downward adjacent to the headwall to a depth equal to the maximum depth of scour. Therefore, the headwall should extend below the maximum expected depth of scour to prevent the headwall from being undermined.

For the gravel and cohesive material, the dimensionless scour-hole profiles revealed that the maximum depth of scour occurs at a distance ranging from $0.30L_{sm}$ to $0.45L_{sm}$ downstream from the culvert outlet. Scour occurs directly under the culvert outlet to a depth of approximately $0.4d_{sm}$. The sidewall slope of the scour cavity is considerably steeper on the culvert side than it is on the opposite side where the water jet impacts.

Mound Geometry

One component of the local scour process near a culvert outlet is the formation of an aggraded mound downstream of the scour area. The mound dimensions of height (h_m), width (W_m), and length (L_m) were correlated with DI by normalizing mound dimensions in terms of the culvert diameter (D). Logarithmically plotting the mound dimensionless parameters versus the DI yields a series of linearized relationships. Fitting a power regression equation through each set of data yields a general equation of the following form:

$$\text{Maximum mound dimension}/D = (DI)^b \quad (10)$$

where the maximum mound dimension is height, width, or length and a and b are curve coefficients.

Figure 9 shows that after 316 min the height, width, and length of the mound can be correlated with the DI when the tailwater is set at 0.45D. The equation coefficients are as follows:

Mound Dimension	a	b
h_m	0.34	0.73
W_m	21.19	1.05
L_m	15.22	0.90

It is evident that the mound geometry can be described as a function of the culvert hydraulics for a uniformly graded sand material.

Relation Between Mound Geometry and Scour-Hole Dimensions

Relationships correlating the geometric characteristics of the scour hole with corresponding dimensions of the mound were derived. The general equation describing this relationship can be expressed in the following general form:

$$\text{Maximum mound dimension}/D = c\,(\text{maximum scour-hole dimension}/D)^d \quad (11)$$

where the maximum scour-hole dimensions are depth, length, and width; the maximum mound dimensions are height, width, and length; and c and d are curve coefficients. The resulting correlation coefficients are summarized below:

Mound Dimension	Scour-Hole Dimension	c	d
Height	Depth	0.10	1.52
Width	Width	0.55	1.47
Length	Length	1.83	0.78

There exists a direct proportionality between mound dimensions and scour-capacity dimensions at the equilibrium stage. For example, the mound height is generally 10 to 15 percent of the scour-hole depth when the culvert is flowing less than full. However, the mound height elevates to approximately 20 percent of the scour-hole depth when the

Figure 7. Comparison of scour-hole characteristics with and without headwall for uniform sand.

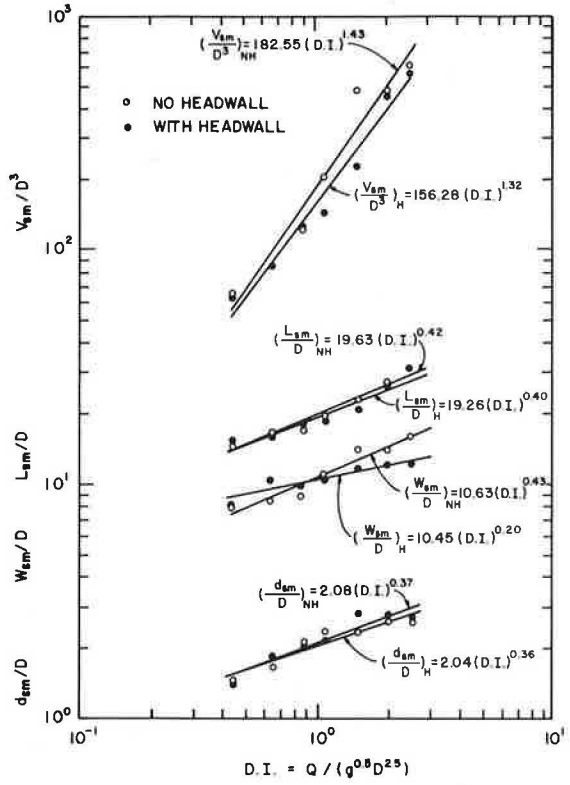

culvert flows full. These relationships permit the estimation of the extent of mound deposition due to localized scour in a sand material.

Scour Influence

The scour mechanism was found to affect areas downstream of the scour hole through the deposition of scoured materials. The length of scour influence (SI) is defined as the length of the scour hole (L_{sm}) plus the length of the mound deposition (L_{mm}). The width of SI is the width of the mound deposition. In order to quantify the SI tests were performed in uniform sand to document the extent of mound movement.

Figure 10 shows the relationship found between DI and the maximum length and maximum width of SI expressed in culvert diameters. An analysis indicates that the length of the mound is approximately the same as the maximum length of the scour hole for a culvert flowing full. The length of SI is twice the length of the scour hole measured downstream from the culvert outlet. It was observed that the width of SI ranges from two to three times the scour-hole width for DIs of 1.0 to 3.0. The SI influence relationships apply to culverts flowing full.

The total area affected by the local scour and deposition process, the SI area (A_{SI}), can be estimated as

$$A_{SI} = (L_{sm} + L_{mm}) \times W_{mm} \quad (12)$$

where W_{mm} is the maximum mound width. When the length and width components in Equation 12 are replaced by the function presented in Figure 10, A_{SI} can be approximated as

$$A_{SI} = 672.4\ D^2\ (DI)^2 \quad (13)$$

Therefore, A_{SI} can be depicted in a sand material as a function of the hydraulic characteristics.

CONCLUSIONS

Based on the results obtained through the extensive experimental program described in this paper, it was determined that scour-hole depth, width, length, and volume can be predicted for a noncohesive bed material. The rate of scour was also quantified and observed to reach approximately 80 percent of the maximum scour-hole dimensions after the initial 31 min of testing. The maximum scour depth was located at a point approximately 0.3 to 0.4 the maximum length of scour measured downstream of the culvert outlet.

Tests were performed in noncohesive bed material to measure the effectiveness of a headwall placed adjacent to the culvert outlet. The scour-hole dimensions were similar both with and without a headwall. The headwall protected the embankment from undermining as the scour hole extended as far as $0.2L_{sm}$ into the embankment for the no-headwall condition. However, the headwall should extend to a depth greater than the maximum predicted depth of scour to prevent undermining of the culvert and headwall.

The area affected by scour can be predicted for noncohesive bed materials. It was observed that the length of the affected area was approximately twice the length of the scour hole and that the width of the area was approximately two to three times the width of the scour hole for culverts flowing full.

Figure 8. Dimensionless scour-hole profile with and without headwall for uniform sand.

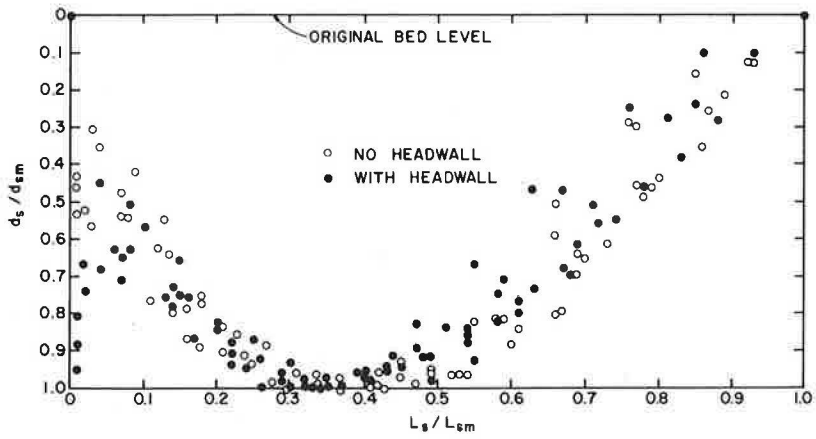

Figure 9. Mound length, width, and height versus DI after 316 min for uniform sand.

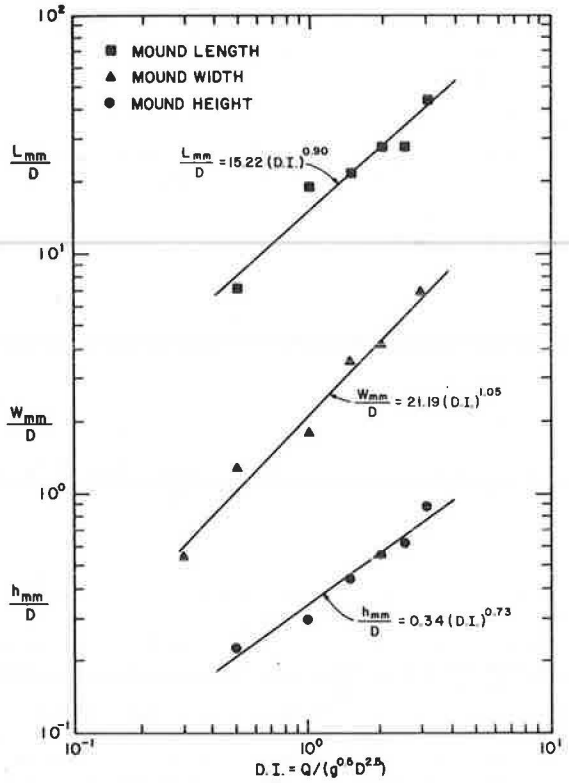

Figure 10. SI versus DI for uniform sand.

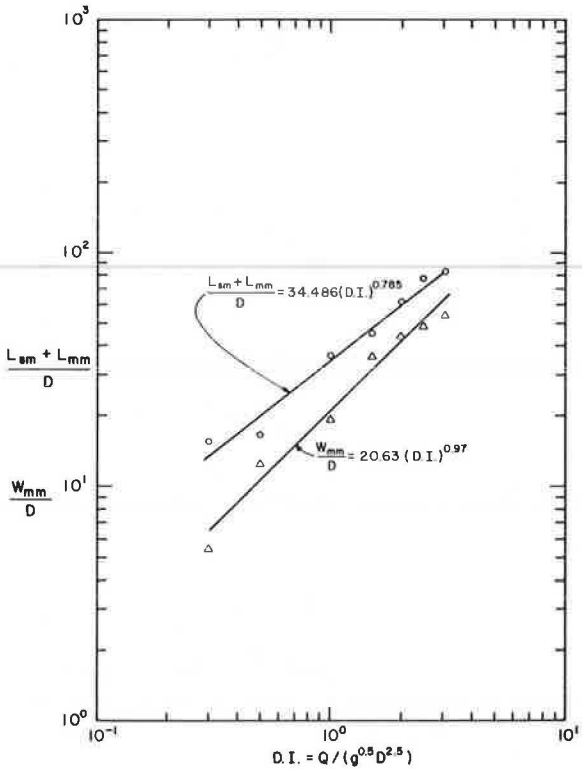

It was determined that the dimensions of scour could be predicted in an SC cohesive soil. Depth, width, length, and volume were correlated with soil saturated shear strength and plasticity index, fluid density and velocity, and time. It was observed that 70 percent of the maximum scour-hole dimensions was reached after the initial 31 min of testing. Furthermore, the maximum scour depth was located at a point approximately 0.35 the maximum length of scour measured downstream of the culvert outlet.

ACKNOWLEDGMENT

This study was conducted at the Engineering Research Center at Colorado State University and was sponsored by the U.S. Department of Transportation (DOT). DOT contract manager J. Sterling Jones provided many useful suggestions for analyzing and presenting the data.

REFERENCES

1. H. Rouse. Criteria for Similarity in the Transportation of Sediment. Proc., 1st Hydraulic Conference, Iowa State Univ., Iowa City, Bull. 20, March 1940, pp. 33-49.
2. E.M. Laursen. Observations on the Nature of Scour. Proc., 5th Hydraulic Conference, June 9-11, 1952.
3. R.A. Thomas. Scour in Gravel Beds. Colorado A&M College, Fort Collins, M.S. thesis, 1953.
4. D.E. Hallmark. Scour at the Base of a Free Overfall. Colorado A&M College, Fort Collins, M.S. thesis, 1955.
5. C. Mendoza. Headwall Influence on Scour at Culvert Outlets. Colorado State Univ., Fort Collins, M.S. thesis, 1980.
6. T.R. Opie. Scour at Culvert Outlets. Colorado State Univ., Fort Collins, M.S. thesis, 1967.
7. J.P. Bohan. Erosion and Riprap Requirements at Culvert and Storm-Drain Outlets. U.S. Army Engineer Waterways Experiment Station, Vicksburg, Miss., Rept. H-70-2, 1970.
8. D. Doddiah. Comparison of Scour Caused by Hollow and Solid Jets of Water. Colorado A&M College, Fort Collins, Master's thesis, 1950.
9. M.A. Stevens. Scour in Riprap in Culvert Outlets. Colorado State Univ., Fort Collins, Ph.D. dissertation, 1969.
10. S.R. Abt and J.F. Ruff. Estimating Culvert Scour in Cohesive Material. Journal of the Hydraulics Division, ASCE, Vol. 108, No. HY1, Proc. Paper 16784, Jan. 1982, pp. 25-34.
11. B.P. Fletcher and J.L. Grace, Jr. Practical Guidance for Design of Lined Channel Expansions at Culvert Outlets. U.S. Army Engineer Waterways Experiment Station, Vicksburg, Miss., Rept. HPR-1 (70-IH), Oct. 1974.

Publication of this paper sponsored by Committee on Hydrology, Hydraulics and Water Quality.